Malaysian Journal of Mathematical Sciences

Journal homepage: https://einspem.upm.edu.my/journal

On Chaos and Multifractality in a Three-Species Food Chain System

Das, S.* and Bhardwaj, R.

University School of Basic Sciences, Guru Gobind Singh Indrapastha University Dwarka, India

E-mail: saureeshdas@gmail.com
**Corresponding author*

Received: 7 March 2019
Accepted: 7 April 2021

Abstract

The complexity of temporal dynamics in the three species food web model involving Holling type-II functional response has been investigated analytically and numerically by varying the kill rate parameter of the super predator. In this work, the system is shown to possess co-existing stable equilibrium population over a certain range of kill rate parameter of the super predator. The transition from stable equilibrium point of coexistence to limit cycle behavior is also observed, at a critical value of the kill rate parameter, as result of Hopf bifurcation. Power spectrum and the bifurcation diagram of the food web system have been used to investigate the transition of the system dynamics from regular to quasi-periodic and chaotic regime for increasing value of the kill rate. Numerical computation of Lyapunov characteristic exponents for specific values of the kill rates provides evidence of chaotic system dynamics or an strange attractor. The chaos in such a system is shown to exhibit scale invariance characteristics as indicated by its fractal dimension. The multi-fractal behavior is further revealed in the temporal evolution of the system through the existence of power law and other measures of the multi-fractal detrended fluctuation analysis for different values of the kill rates of the super predator.

Keywords: functional response; food web; Hopf bifurcation; chaos; power spectrum; bifurcation diagram; multi-fractal analysis; power law.

1 Introduction

The evolution of any ecosystem is governed by different interactions among the various species in it [28]. The phenomenon of mutual co-existence among species in an ecosystem with fluctuations in species abundance was first discussed mathematically in [23, 43]. The study of dynamic relation between predators and prey is of considerable interest to ecologist [33, 42]. The characteristics of predation and parasitism with the functional responses representing ecological interactions has been investigated earlier. De Angelis et al. discussed the model of tropic interaction in his study [10]. Further Beddington [3] studied the effect of mutual interference on searching efficiency while later Berec [4] analyzed the impact of foraging on predator prey dynamics.

In the last two decades the dynamics of realistic ecological models [22] and complexity of three species food chain model [24] have been analyzed with different types of functional responses [7, 32] to study the effect of various factors such as prey refuge [13]and group defense [34] using latest techniques of non linear analysis [29]. The main advantage of developing the model lies in possibility of simulating evolution of the growth of different species and to study the effect of interaction of different species in the ecosystem on the sustainability of species. Laboratory experiment, on the predator-prey interaction on bacterivorous ciliate and two bacterial prey species, by Becks et al.[2] has also confirmed chaotic behavior in the observed aperiodic population oscillations.

Several studies in the area of physics[6], ecology [31], biology [21, 26], physiology [5, 8], neuro-bioscience [9], environment science[11], economics [25], etc., have also suggested the importance of identifying embedded scale invariant structure- a characteristic property of fractals [27]. Fractal analysis of time series is relatively a new approach to study the chaotic dynamics in evolving systems [37, 45]. In ecology, multi-fractal analysis technique [35, 36] has been applied mainly to characterize species-area and species-abundance relationship in a spatial context. The importance of the study on the fractal properties of time series in ecology has been suggested by [40] in relation to persistence of rare species. Complexity of hierarchically generated patterns over distinct time scale in ecology can be resolved by accurate modeling of temporal patterns in time series [1, 40]. Fractal analysis has been used recently to understand complex animal behavior and their conservation- particularly in relation to marine mammals [1, 38].

The investigation of the dynamical complexity of three-species continuous-time food chain, involving Holling type-II [16] functional response, by Hasting and Powell [15] revealed chaotic oscillations in the food web model. The model [15] was further shown to exhibit chaotic dynamics on varying the mortality rate of the predator at the middle level [39]. As the predation rate plays an important role in controlling population of species at different levels, it is important to study the model evolution with varying attack/ kill rate at higher trophic [2, 27].

We therefore revisit the basic food web chain model [15] with a view to understand the global dynamical complexities of the system as a result of varying the attack/ kill rate of the super predator and also the coexistence of species. We carried out extensive numerical simulation of model equations for different attack/ kill rate of the super predator and analyze the simulated data on species population using power spectrum, bifurcation diagram and phase portrait. Beside the linearly stable equilibrium points for coexistence of the species, Hopf bifurcation is shown to occur in the system resulting in a limit cycle behavior. Further, computation of phase portrait and power spectrum for different values of a_2 suggests a quasi-periodic route to chaos in the system. In addition, to quantify the chaos that results on varying the attack/ kill rate in the model, the spectrum of Lyapunov characteristic exponents (LCEs) have been computed [44]. It is shown that a range of attack/kill rate parameter exists for which the phase space attractor of the present

three species food web model evolves to a strange attractor and limit cycles. Fractals exhibiting self similar structure or single scaling rule are termed as mono-fractal whereas multi-fractals follows multiple scaling rules and scale dependent dimensions. The MFDFA method [19, 41] used in the analysis allows for q- order extension of overall root mean square (RMS) amplitude fluctuation (F_q), and leads to a power-law relation characterized by the q dependent Hürst exponent(H_q). The observed decreasing trend of H_q, in the plot of H_q versus q captures the inherent multi-fractal behavior. The fractal analysis of the time series obtained in the foregoing three species food web model, further reveals the presence of multiple scaling exponents in their singularity spectrum- a characteristic of multi-fractal behavior.

2 Mathematical Formulation of the Three-Species Food Chain Model

A simple mathematical model of vertical three species food web structure, involving the number X(prey) of species at the lowest level which are preyed upon by Y(predator)- the number of species at the next higher level and Z(top predator)- the number of species at the top level which preys upon Y may be written as [15],

$$\frac{dX}{dT} = R_0 X\left(1-\frac{X}{K_0}\right) - C_1 F_1(X)Y, \tag{1}$$

$$\frac{dY}{dT} = F_1(X)Y - F_2(Y)Z - D_1 Y, \tag{2}$$

$$\frac{dZ}{dT} = C_2 F_2(Y)Z - D_2 Z, \tag{3}$$

where R_0, K_0, ${C_1}^{-1}$ and C_2 refer to intrinsic growth rate of X, carrying capacity of X, conversion rate of prey to predator for species Y and conversion rate of prey to predator for species Z respectively. In addition, D_1 and D_2 are the mortality rate of the predator Y and the predator Z respectively. Following [33, 15], the functional responses are considered to be of Holling type II i.e., $F_i(U) = \frac{A_i U}{B_i + U}$, i = 1,2 with A_i representing the asymptotic predator killing rate and B_i are constants that correspond to the prey population level when killing rate per unit prey is half its maximum value i.e., $[F_1(X)]_{X=B_1} = \frac{A_1}{2}$ and $[F_2 Y]_{Y=B_2} = \frac{A_2}{2}$.

Eq.(1)-(3) may be reduced to the following non-dimensional form,

$$\frac{dx}{dt} = x\,(1-x) - f_1\,(x)\,y, \tag{4}$$

$$\frac{dy}{dt} = f_1\,(x)\,y - f_2\,(y)\,z - d_1 y, \tag{5}$$

$$\frac{dz}{dt} = f_2\,(y)\,z - d_2 z, \tag{6}$$

by substituting $x = \frac{X}{K_0}$, $y = \frac{C_1 Y}{K_0}$, $z = \frac{C_1 Z}{C_2 K_0}$ and $t = R_0 T$. The functional responses $F_i(U), i = 1$, 2 may be rewritten in terms of new variables as:

$$f_i\,(u) = \frac{a_i u}{(b_i + u)}. \tag{7}$$

The reduced form of the three species food web model i.e., eq.(4)-(7) involves only six parameters namely d_i, a_i, and b_i $(i = 1, 2)$ which correspond to the non-dimensional mortality rates, attack/ killing rates (hereafter referred to as kill rate) and prey population levels respectively.

It is observed that the system admits four non-negative equilibrium points $E_j(x_0, y_0, z_0), j = 1, \cdots, 4$, [20, 33] which are given as,

$$\begin{aligned} E_1(x_0, y_0, z_0) &= [0, 0, 0], \\ E_2(x_0, y_0, z_0) &= [1, 0, 0], \\ E_3(x_0, y_0, z_0) &= \left[\frac{d_1}{(a_1 - d_1 b_1)}, \frac{a_1 - d_1 - d_1 b_1}{(a_1 - d_1 b_1)^2}, 0\right], \\ E_4(x_0, y_0, z_0) &= \left[x_0, \frac{d_2}{(a_2 - b_2 d_2)}, \frac{x_0(a_1 - b_1 d_1) - d_1}{(1 + b_1 x_0)(a_2 - b_2 d_2)}\right], \end{aligned} \tag{8}$$

where in $E_4(x_0, y_0, z_0)$ we have $x_0 = \frac{b_1 - 1}{2b_1} + \frac{1}{2b_1}\sqrt{(b_1 + 1)^2 - \frac{4b_1 a_1 d_2}{a_2 - b_2 d_2}}$.

The linear stability of the above equilibrium points can be analyzed using the following Jacobian of the system,

$$J(x, y, z) = \begin{bmatrix} xF_{1x} + F_1 & xF_{1y} & xF_{1z} \\ yF_{2x} & yF_{2y} + F_2 & yF_{2z} \\ zF_{3x} & zF_{3y} & zF_{1z} + F_3 \end{bmatrix}, \tag{9}$$

where $F_1 = \left[(1 - x) - \frac{a_1 y}{1 + b_1 x}\right]$, $F_2 = \left[\frac{a_1 x}{1 + b_1 x} - \frac{a_2 z}{1 + b_2 y} - d_1\right]$ and $F_3 = \left[\frac{a_2 y}{1 + b_2 y} - d_2\right]$.

The equilibrium point $E_1(x_0, y_0, z_0) = [0, 0, 0]$ is always unstable as the eigenvalues of the Jacobian matrix are $1, -d_1$ and $-d_2$ respectively. Similarly for the condition that $\frac{a_1}{d_1(1 + b_1)} < 1$, the equilibrium point $E_2(x_0, y_0, z_0) = [1, 0, 0]$ is locally asymptotically stable.

In case of the equilibrium point $E_3(x_0, y_0, z_0) = \left[\frac{d_1}{(a_1 - d_1 b_1)}, \frac{a_1 - d_1 - d_1 b_1}{(a_1 - d_1 b_1)^2}, 0\right]$ corresponding to absence of the super-predator z, the asymptotic stability occurs for the case of $\frac{a_1 b_1 y_0}{(1 + b_1 x_0)^2} < 1$ and $\frac{a_2 y_0}{d_2(1 + b_2 y_0)} < 1$.

For the co-existence of the species, considering only the positive interior equilibrium solution denoted as E_4 above, we find that the the Jacobian matrix at this equilibrium point may be written as,

$$J(x_0, y_0, z_0) = \begin{bmatrix} P_{11} & P_{12} & P_{13} \\ P_{21} & P_{22} & P_{23} \\ P_{31} & P_{32} & P_{33} \end{bmatrix}, \tag{10}$$

where $P_{11} = -x_0 + \frac{a_1 b_1 x_0 y_0}{(1 + b_1 x_0)^2}$, $P_{12} = -\frac{a_1 x_0}{(1 + b_1 x_0)}$, $P_{13} = 0$, $P_{21} = \frac{a_1 y_0}{(1 + b_1 x_0)^2}$, $P_{22} = \frac{a_2 b_2 y_0 x_0}{(1 + b_2 y_0)^2}$, $P_{23} = -\frac{a_2 y_0}{(1 + b_2 y_0)}$, $P_{31} = 0$, $P_{32} = \frac{a_2 z_0}{(1 + b_2 y_0)^2}$ and $P_{33} = 0$.

The characteristic equation can therefore be written as,

$$\lambda^3 + \sigma_1 \lambda^2 + \sigma_2 \lambda + \sigma_3 = 0, \tag{11}$$

where $\sigma_1 = -(P_{11} + P_{22})$, $\sigma_2 = (P_{11}P_{22} - P_{12}P_{21} - P_{23}P_{32})$ and $\sigma_3 = P_{11}P_{23}P_{32}$. Thus based on Routh-Hurwitz criteria, the equilibrium point is locally asymptotically stable if $\sigma_1 > 0, \quad \sigma_3 > 0$ and $\sigma_1\sigma_2 > \sigma_3$. On violation of these conditions, the system evolves to a nonlinear regime where bifurcation phenomenon and chaos are observed.

Of the six parameters characterizing the system eq.(4)-(7), we investigate its global complex dynamics by varying the kill rate parameter a_2 of the super-predator while keeping the values of other biological parameters of the system same as in [15, 33, 39]. The parameters values are therefore $a_1 = 5.0,\ b_1 = 3.0,\ b_2 = 2.0,\ d_1 = 0.40$ and $d_2 = 0.01$.

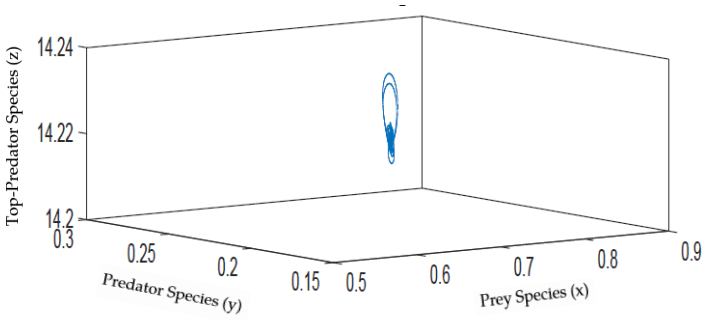

Figure 1: Phase portrait for the system at $a_2 = 0.070$ with $a_1 = 5.0, b_1 = 3.0, b_2 = 2.0, d_1 = 0.4$, and $d_2 = 0.01$.

In the present work, we observe that for $0.0602 \leq a_2 \leq 0.07543$, stable positive equilibrium solutions for co-existence are possible. For the attack/ kill rate $a_2 = 0.070$, we obtain the fixed point solution for the system eq.(4)-(7), as $x_0 = 0.6666$, $y_0 = 0.2000$ and $z_0 = 14.2222$ (Fig.1). The steady state solution is observed to be linearly stable since $\sigma_1 = 0.2413$, $\sigma_2 = 0.0382$ and $\sigma_3 = 0.0023$ are such that the condition $\sigma_1.\sigma_2 > \sigma_3$ for asymptotic stability is satisfied.

3 Numerical Simulation of Complex Dynamics

In this section we present the results of numerical simulation of the three species food chain for different values of the kill rate parameter a_2.

3.1 Quasi-Periodic Motion Leading to Chaos

Beside the range of values of the parameter a_2 for which stable fixed point for the species to coexist, we also observe a Hopf-bifurcation (stable equilibrium point $\rightarrow$ stable limit cycle) in the system, say for $a_2 = 0.07546$ (Fig. 2a). Based on discrete Fourier transform (DFT) method [11], the power spectrum of the time series of the species Z for different values of a_2 have also been computed to analyze the frequency distribution. For the parameter $a_2 = 0.07546$, the power spectrum for the limit cycle, shown in Fig. 2b, exhibit the presence of only one frequency. Subsequently,

at $a_2 = 0.07708$ the phase portrait and the corresponding power spectrum show the transition to quasi-periodic dynamics (Fig. 2c,d). Increasing the value of the control parameter a_2 to 0.0800, the dynamics of the system switches to chaos (Fig. 2e,f). Therefore the increase of the kill rate parameter a_2 has been found to introduce unstable equilibrium points into the system dynamics thus causing an extensive changes in the attractor dynamics which could be chaotic or at times quasi-periodic as revealed in the following power spectrum (Fig. 4a-f).

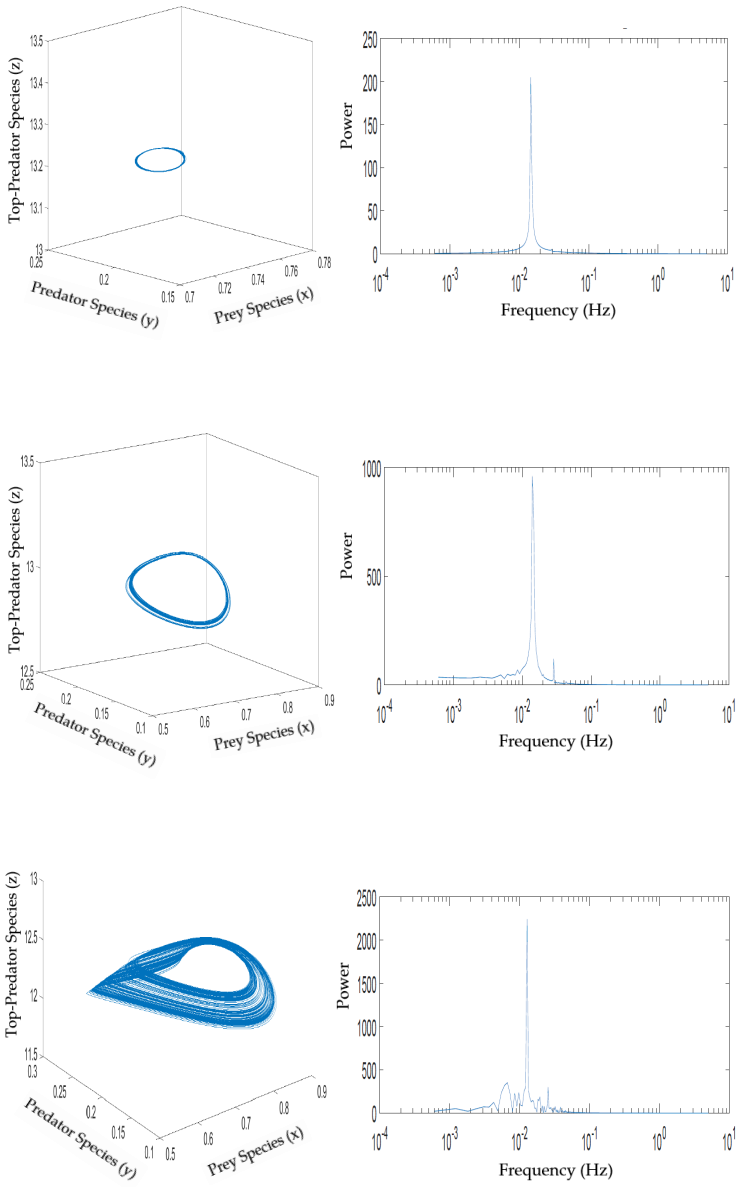

Figure 2: a)Phase portrait for the system at $a_2 = 0.07546$, b) Power spectra for the time series Z at $a_2 = 0.07546$, c)Phase portrait for the system at $a_2 = 0.07708$, d) Power spectra for the time series Z at $a_2 = 0.07708$, e)Phase portrait for the system at $a_2 = 0.08000$, f)Power spectra for the time series Z at $a_2 = 0.08000$ with $a_1 = 5.0$, $b_1 = 3.0$, $b_2 = 2.0$, $d_1 = 0.4$, and $d_2 = 0.01$.

3.2 Bifurcation Diagram and Spectral Analysis

Emergence of chaos is closely related to the existence of bifurcation. A bifurcation of a dynamical system occurs when the phase portrait changes its topological structure for some value of the control parameter. Similarly, the power spectra of a time series provides the distribution of power into various frequency component. For the nonlinear three-species model eq.(4)-(7), we have computed the bifurcation diagram by plotting the successive maxima of the predator population Z with increased killing rate a_2 (Fig. 3). Since no significant change in the bifurcation plot is observed in between $a_2 = 1.1$ and $a_2 = 1.5$, the maximum value for a_2 is set to 1.5. The bifurcation diagram exhibit complex chaotic dynamics over considerable range of killing rate of the predator Z. However, the bifurcation diagram also shows several windows over which the system dynamics could be regular. For $a_2 = 0.10$, the bifurcation diagram exhibit chaotic dynamics as also illustrated in the corresponding power spectrum (Fig. 4a). With increase in the value of a_2, the system dynamics continues to be chaotic till $a_2 = 0.2480$ where quasi-periodic motion sets in (Fig. 4c). The power spectrum of Fig. 4d-f, belonging to the range $0.20 \leq a_2 \leq 0.60$ of the bifurcation diagram, illustrates the occurrence of several new time scales into the three species food chain. Similarly, the bifurcation diagram for different values of a_2 in the range $0.60 \leq a_2 \leq 1.5$ exhibit complex dynamics i.e. chaos, noisy quasi-periodic and limit cycle behavior as revealed in the phase diagrams (Fig. 5a-d).

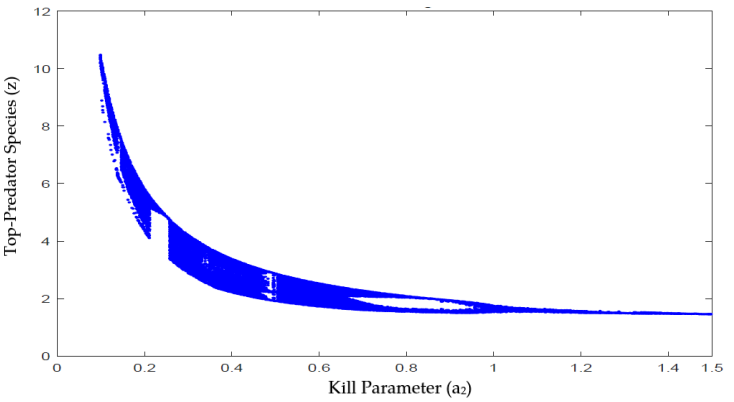

Figure 3: Bifurcation diagram of the system for variation of kill rate a_2 with $a_1 = 5.0, b_1 = 3.0, b_2 = 2.0, d_1 = 0.4$, and $d_2 = 0.01$.

3.3 Characterization of Dynamical Complexity Using Lyapunov Exponents

In the foregoing, we studied the complex dynamics exhibited by the tritrophic food web model i.e., eq.(4)-(7), as the killing rate parameter a_2 is increased. The bifurcation diagram (Fig. 3) clearly shows the range of values of a_2 for which the system exhibit chaotic behavior. The spectrum of Lyapunov characteristic exponents (LCEs) for a dynamical system further quantifies the prevailing chaotic system dynamics. The LCEs are asymptotic measures characterizing the average exponential rate of divergence/ convergence of small perturbations in the phase space. For a continuous 3-dimensional dissipative system, the attractor in the phase space is characterized by the spectrum of LCE's which involve three exponents $(\lambda_1, \lambda_2, \lambda_3)$. The attractor in the phase space is termed as a *strange attractor*, *two-torus*, *limit cycle* and *fixed point*, if the LCE's are of the form $(+, 0, -)$, $(0, 0, -)$, $(0, -, -)$ or $(-, -, -)$ respectively.

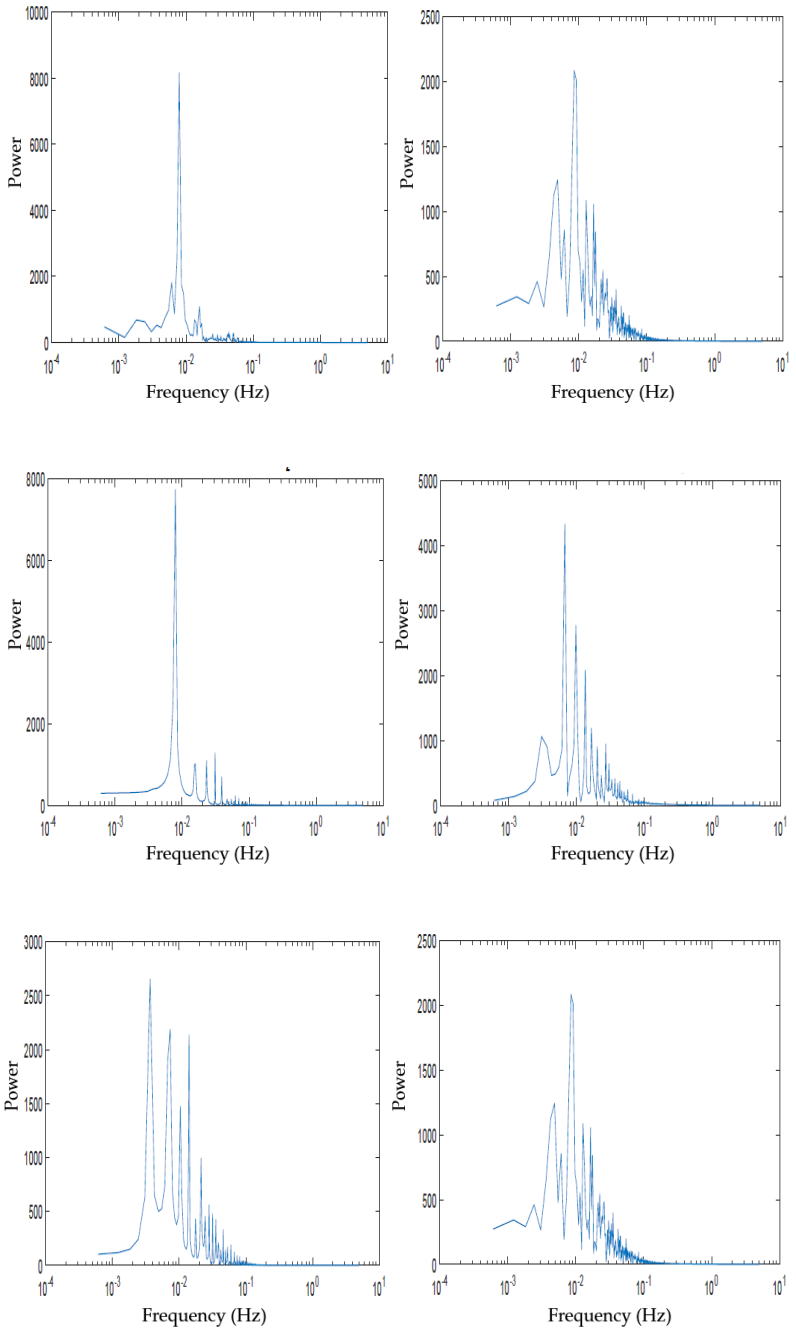

Figure 4: Power spectra of the time series Z for a)$a_2 = 0.10$, b)$a_2 = 0.20$, c)$a_2 = 0.2480$, d)$a_2 = 0.30$, e)$a_2 = 0.4951$, f)$a_2 = 0.60$ with $a_1 = 5.0$, $b_1 = 3.0$, $b_2 = 2.0$, $d_1 = 0.4$, and $d_2 = 0.01$.

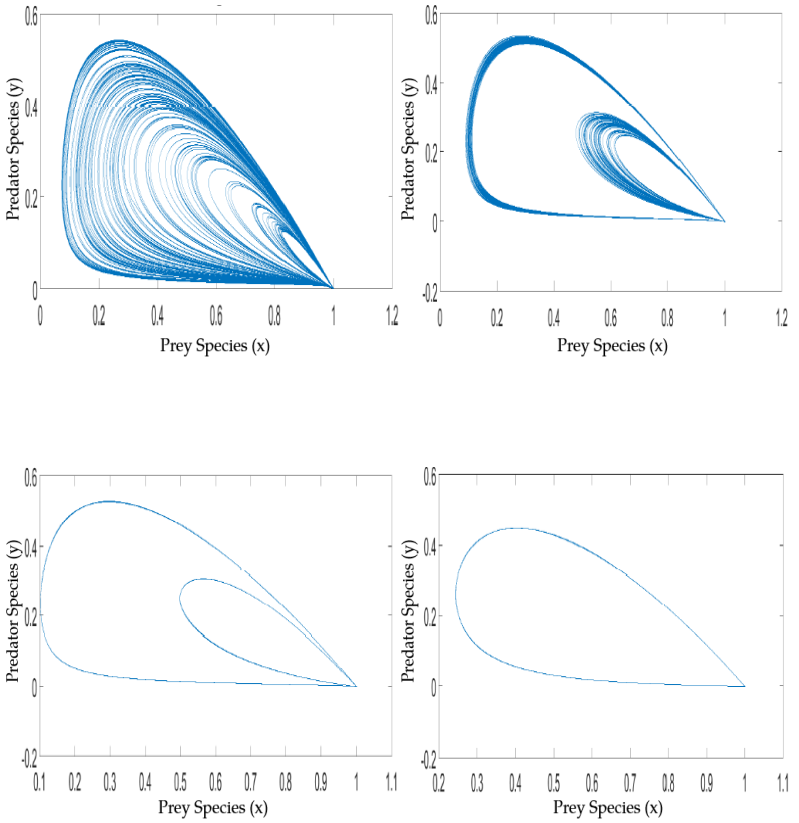

Figure 5: x-y plot for the system for a)$a_2 = 0.60$, b)$a_2 = 0.80$, c)$a_2 = 0.8748$, d)$a_2 = 1.301$ with $a_1 = 5.0$, $b_1 = 3.0$, $b_2 = 2.0$, $d_1 = 0.4$, and $d_2 = 0.01$.

An attractor with a positive LCE corresponds to exponential divergence of two trajectories with almost same initial condition and further results in unpredictable long term dynamics i.e., chaos, due to stretching and folding in phase space. The negative LCE correspond to a stable periodic dynamics in phase space. Denoting the length of the principal axis of an ellipsoid as d_i, $i = 1, 2, 3 \cdots$, we define the *i*-th one dimensional LCE as:

$$\lambda_i = \lim_{t \to \infty} \frac{1}{t} log_2 \left(\frac{d_i(t)}{d_0} \right), \tag{12}$$

where t refers to time. The exponents have been computed in bits per unit time using the Wolf et al.[44] algorithm. The algorithm has been run for different values of kill rate parameter a_2 with time step size 0.01 and the asymptotic values of LCE's are determined when $t = 10000$. For the chaotic behavior of the system, the largest of the LCE's $\lambda_i, i = 1, 2, 3$ must be positive. The qualitative behavior of complex system dynamics, as observed in the bifurcation diagram (Fig. 3), is further quantified using the largest LCE computed for different a_2. Fig. 6 illustrates the variation of largest LCE with the increase in kill rate parameter a_2.

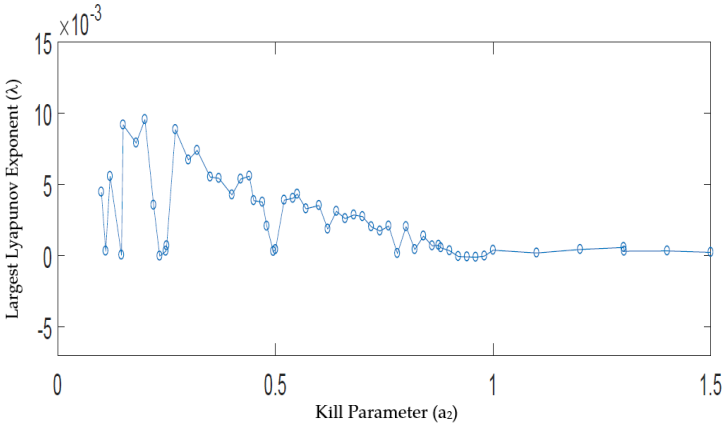

Figure 6: Variation of largest Lyapunov exponent with killing rate parameter a_2.

In the present work, when the control parameter a_2 is varied in the range $0.10 \leq a_2 \leq 0.20$, with $a_1 = 5.0$, $b_1 = 3.0$, $b_2 = 2.0$, $d_1 = 0.4$, and $d_2 = 0.01$ in the system eq.(4)-(7), the spectrum of LCE's are observed to converge to a form $(+, 0, -)$. For example, for

$$\begin{aligned} a_2 = 0.10 : \lambda_1 &= 0.004464, \quad \lambda_2 = 0.000252 \quad \text{and} \quad \lambda_3 = -0.345645, \\ a_2 = 0.18 : \lambda_1 &= 0.007906, \quad \lambda_2 = 0.000278 \quad \text{and} \quad \lambda_3 = -0.693363, \\ a_2 = 0.20 : \lambda_1 &= 0.009555, \quad \lambda_2 = 0.000178 \quad \text{and} \quad \lambda_3 = -0.725519. \end{aligned}$$

Therefore, the system exhibit *strange attractor / chaos* in such a range of values for a_2. Fig.7 illustrates the time variation of LCE's for the case of $a_2 = 0.20$. In addition the LCE's, for which the system show *quasi-periodic / limit cycle* behavior for different values of a_2, are:

$$\begin{aligned} a_2 = 0.2480 : \lambda_1 &= 0.000315, \quad \lambda_2 = -0.005783 \quad \text{and} \quad \lambda_3 = -0.758837, \\ a_2 = 0.4951 : \lambda_1 &= 0.000300, \quad \lambda_2 = -0.000655 \quad \text{and} \quad \lambda_3 = -0.887539, \\ a_2 = 0.8748 : \lambda_1 &= 0.000733, \quad \lambda_2 = -0.000837 \quad \text{and} \quad \lambda_3 = -0.930543, \\ a_2 = 1.3010 : \lambda_1 &= 0.000314, \quad \lambda_2 = -0.002750 \quad \text{and} \quad \lambda_3 = -0.951582, \end{aligned}$$

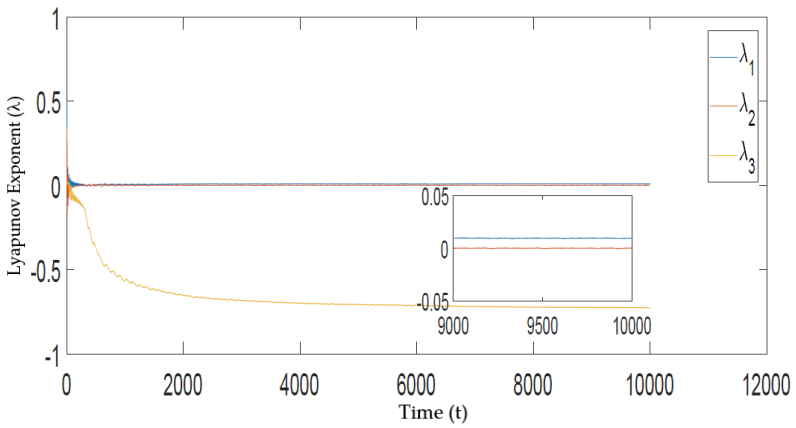

Figure 7: Lyapunov exponents for the three-species food web for kill rate parameter $a_2 = 0.20$ with $a_1 = 5.0$, $b_1 = 3.0$, $b_2 = 2.0$, $d_1 = 0.4$, and $d_2 = 0.01$. The inset illustrates the details of convergence of λ_1 and λ_2.

4 Multi-Fractal Analysis

A time series $X(t)$ is said to be self similar or scale invariant if $X(at) = a^H X(t)$, where H is the scaling exponent also called Hürst exponent. Similarly, if an object breaks into smaller parts of itself but retaining its shape / structure, the object is termed as fractal, if its dimension is non-integer. The fractal behavior of population time series of bird species having almost same average abundance has been studied in [40]. The American redstart time series is shown to have fractal dimension 1.62 while that of least flycatcher population time series 1.44, thereby suggesting that the former species is prone to local extinction. It is noted that the changes in the self similarity or scale invariance parameter of certain biomedical time series may reflect the transition to improved pathological conditions [14]. Recently, fractal analysis has been applied to detect time-invariant scaling in daily catch time series of smooth pink shrimp from the west coast of Vancouver Island [30]. In ecology the fractal approach may provide valuable information about inherent mechanism driving the ecological systems and origin of complexity in the system may be linked to understanding the origin of fractal scaling [12, 30, 31, 35, 40]. The self-similarity property of fractals simplify substantially the ecological modeling of the phenomenon. Fractal approach provides a tool to qualitatively describe objects that are extremely disordered and complex. Therefore it is important to extend the study of dynamics of ecological systems to fractal analysis of the biological time series obtained from these ecological models [12, 31]. But many time series do not exhibit simple mono-fractal scaling behavior which can be accounted by single scaling exponent [17]. In such cases multitude of scaling exponents is required for a full description of scaling behavior and a multi-fractal analysis must be employed.

4.1 Multi-Fractal Detrended Fluctuation Analysis

In this section, MFDFA [19] has been adopted to investigate the scale invariance characteristics of the time series of species X of the tritrophic model eq.(4)-(7), for different kill rate parameter a_2.

We briefly outline below the various steps involved in the multi-fractal procedure to determine different scales embedded in the time series of the species X.

Step 1: For the time series $X = \{x_k,\ k = 1,\ \cdots N\}$, the profile $\mathcal{Y}(i)$ is first constructed as:

$$\mathcal{Y}(i) \equiv \sum_{k=1}^{N} [x_k - < x >]; i = 1, 2, 3, \cdots, \tag{13}$$

Step 2: The profile is divided into non-overlapping segment of equal length s (scale). In case the time series length N is not an exact multiple of s, then in order to consider the data points in the remaining part, the profile is divided from the opposite end to give $2N_s$ segments in all.

Step 3: Find the local trend for each of the $2N_s$ segments by a least-square fit . The variance is determined as:

$$F^2(\nu, s) = \frac{1}{s} \sum_{i=1}^{s} \{\mathcal{Y}[(\nu - 1)s + i] - y_\nu(i)\}^2, \tag{14}$$

for each segment $\nu = 1, 2, 3, \cdots, N_s$. The variance for each of the segment $\nu = N_s + 1, \cdots, 2N_s$ is given by:

$$F^2(\nu, s) = \frac{1}{s}\sum_{i=1}^{s}\{\mathcal{Y}[N - (\nu - N_s)s + i] - y_\nu(i)\}^2, \tag{15}$$

where $y_\nu(i)$ is the local polynomial fitted to the data segment ν.

Step 4: Averaging over all the segments results in q-th order fluctuation function

$$F_q(s) = \left\{\frac{1}{2N_s}\sum_{\nu=1}^{2N_s}[F^2(s,\nu)]^{q/2}\right\}^{1/q} \quad \text{for} \quad q \neq 0, \tag{16}$$

is obtained. Here the index variable q can assume any real value. Also eq.(16) provide standard DFA analysis for $q = 2$. Further, the fluctuation function $F_q(s)$ for $q = 0$ may be written as [19],

$$F_0(s) = \exp\left\{\frac{1}{4N_s}\sum_{\nu=1}^{2N_s}\ln[F^2(\nu, s)]\right\}. \tag{17}$$

For a given value of q, the generalized fluctuation function $F_q(s)$ is computed for different time scale s.

Step 5: Plot of $\log(F_q(s))$ vs $\log(s)$ determines the scaling behavior of the fluctuation. For the time series $\{x_k,\ k = 1,\ \cdots N\}$ to be long-range power-law correlated, the fluctuation function scales as,

$$F_q(s) \sim s^{H_q}, \tag{18}$$

where H_q defines the q-th order Hürst exponent or generalized Hürst exponent. For positive q, the average fluctuation function $F_q(s)$ is dominated mostly by the large variance $F^2(\nu, s)$. Therefore H_q corresponds to the scaling behavior with large fluctuations for positive values of q. In a similar way H_q with negative q describes the scaling behavior of segments with smaller fluctuations. Thus for a time series, if H_q varies with q, it is termed as multi-fractal whereas if H_q remains constant as q is changed, the time series is mono-fractal.

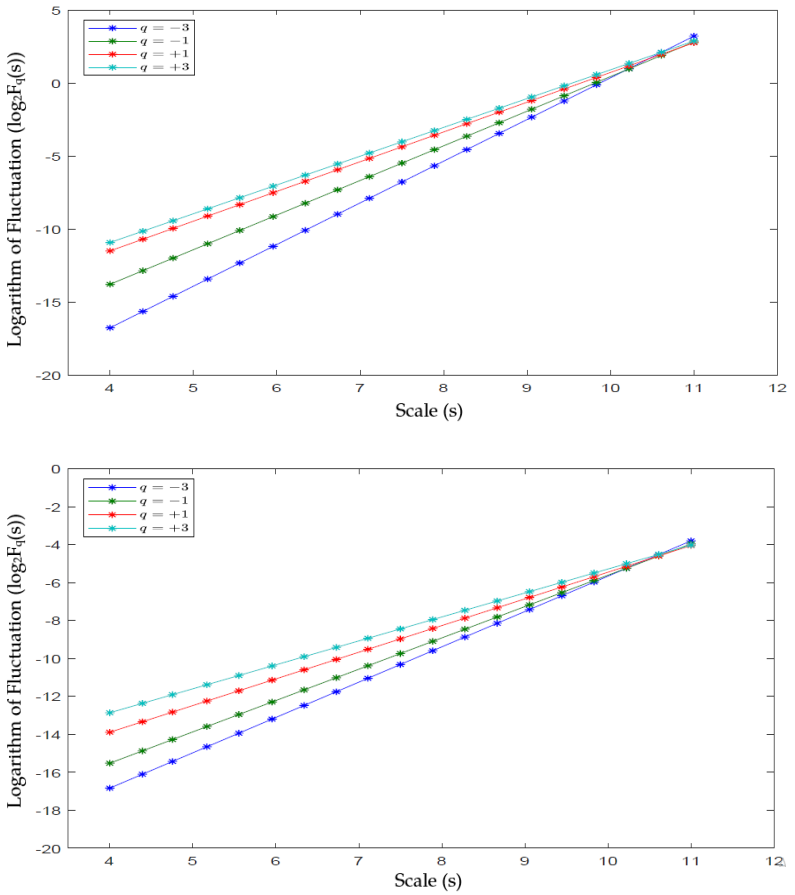

Figure 8: The q-th order root mean square fluctuation F_q verses scale s for (a) $a_2 = 0.10$, (b) $a_2 = 0.60$, with $a_1 = 5.0,\ b_1 = 3.0,\ b_2 = 2.0,\ d_1 = 0.4$, and $d_2 = 0.01$.

In parameterizing the multi-fractal structure of a time series, the q-th order Hürst exponent H_q is only one type of several types of scaling exponents. The generalized Hürst exponent H_q is also related to q-order mass exponent or scaling exponent t_q as,

$$t_q = qH_q - 1. \tag{19}$$

Since H_q is a constant for mono-fractal time series, t_q varies linearly with q. For multi-fractal behavior, t_q varies nonlinearly with H_q.

Other measures of multi-fractal behavior of a time series are singularity exponent or Hölder exponent h_q and singularity dimension D_q and are defined as,

$$\begin{aligned} h_q &= t_q^{'}, \\ D_q &= qh_q - t_q. \end{aligned} \tag{20}$$

The parameters h_q and D_q are also termed as singularity strength α and singularity spectrum $f(\alpha)$ respectively in [38].

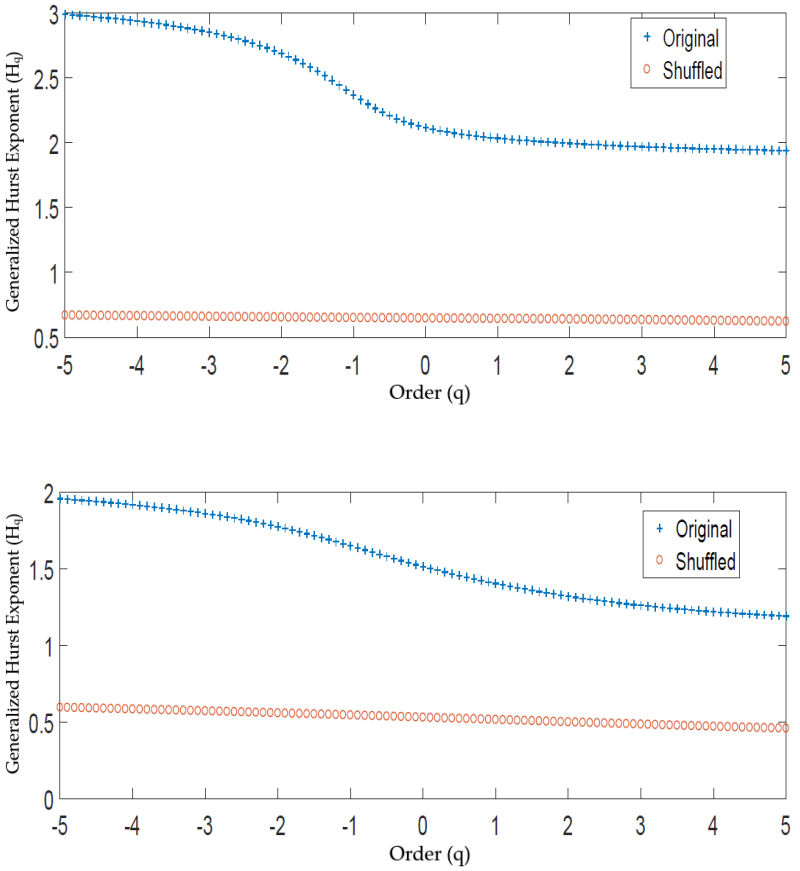

Figure 9: Variation of the generalized Hürst exponent H_q for the original time series (*blue*) and shuffled time series (*magenta*) with order q for (a) $a_2 = 0.10$, (b) $a_2 = 0.60$, with $a_1 = 5.0,\ b_1 = 3.0,\ b_2 = 2.0,\ d_1 = 0.4$, and $d_2 = 0.01$.

4.2 Multi-Fractality in Three-species Food Web Model

In our multi-fractal analysis, we choose the chaotic time series for the species X of the three-species food web, corresponding to the parameter $a_2 = 0.10$ and 0.60 and refer them as Case-I and Case-II respectively. In Fig. 8(a,b), the plot between q-th order RMS fluctuations $F_q(s)$ and the scale s, for Case-I and II respectively clearly shows change in values of slope of regression lines with increase in value of q. Therefore the time series in Case-I and Case-II are of multi-fractal nature. Also, the observed linear relationship in Fig. 8(a,b) establishes the long-range power-law in the data for these cases.

A time series is termed as persistent and showing long-memory if the q-th order Hürst exponent $H_q > 0.5$. For $H_q = 0.5$, the time series is completely random. If $H_q < 0.5$, the time series is anti-persistent and exhibit negative autocorrelation. Further, for mono-fractal fractal behavior H_q does not change with the order q while for multi-fractal behavior H_q decreases with order q. For Case-I and II, the plot of q-th order Hürst exponent $H(q)$ with order q, shown in Fig. 9(a,b), therefore provide evidence for the multi-fractal nature of the biological time series [12, 17, 30]. A random shuffling of the time series results in uncorrelated data for which the Hü rst exponent

H_q remains constant as also shown in Fig. 9(a,b). For Case-I and II, we find that $H_2 = 1.996$ and $H_2 = 1.323$ respectively. Since the values exceed 0.5, both the time series are non-stationary and exhibit long-range power-law correlation. Therefore both time series of the species X are positively correlated in a power-law fashion.

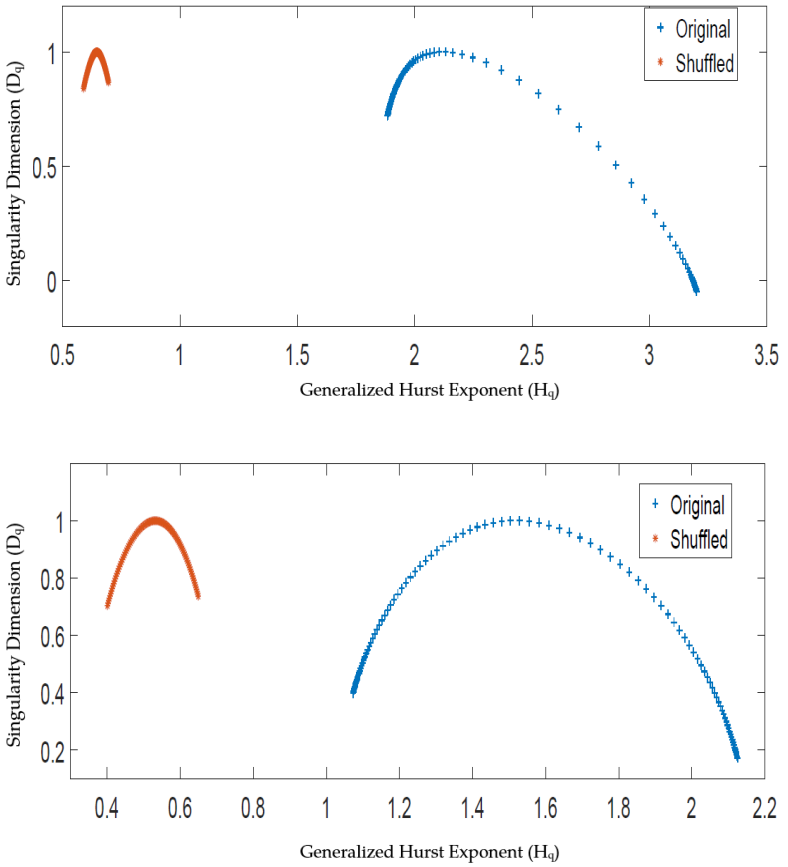

Figure 10: Singularity spectrum $D_q - H_q$ for original time series (*blue*) and shuffled time series (*magenta*) for (a) $a_2 = 0.10$, (b) $a_2 = 0.60$, with $a_1 = 5.0,\ b_1 = 3.0,\ b_2 = 2.0,\ d_1 = 0.4$, and $d_2 = 0.01$.

Using eq.(19)-(20), the mass exponent (t_q), the singularity or Hölder exponent (h_q) and the singularity spectrum (D_q) are computed. For mono-fractals, the shape of singularity spectrum is a point while it is a humped curve for multi-fractals. The difference between maximum and minimum value of h_q in the singularity spectrum defines the width of the spectrum, Δ_{h_q} and provides the extent of multi-fractality of a time series. On reshuffling the time series , the correlation between the successive data points gets minimized. As a result the width of the singularity spectrum $\Delta_{h_q}^{shuf}$ of reshuffled series is expected to be lower than that of the original time series [18]. Fig. 10(a,b) shows the multi-fractal singularity spectrum for Case-I and Case-II respectively. The results of random shuffling the time series are also shown in these plots (magenta color). Since $\Delta_{h_q} > \Delta_{h_q}^{shuf}$ for both Case-I and Case-II, we conclude that the log-range correlation present in the original time series is responsible for multi-fractal behavior of the species time series X. Similar results are obtained for the corresponding species Y and Z time series.

5 Conclusion

The effect of varying super predator killing rate parameter a_2 on the three species food chain model has been explored analytically and numerically with a view to understand the inherent complex chaotic temporal behavior of the evolution of the species population. We have shown the existence of stable equilibrium point for the coexistence of the three species for the super predator kill rate parameter a_2 lying in the range $0.0602 \leq a_2 \leq 0.07543$. The transition from stable equilibrium state to limit cycle behavior is observed for the kill rate parameter $a_2 = 0.07546$ as a result of Hopf bifurcation of the system. Subsequent increase in a_2 values sets in quasi-periodic and chaotic dynamics in the system as revealed through its respective phase portrait and power spectrum (Fig.2). The dynamical complexity of the system is further investigated using the bifurcation diagram, power spectrum and phase plots which along with the LCE's for different values of the parameter a_2 characterize the system dynamics. Specific values of a_2 are observed for which the system exhibit chaotic dynamics or an strange attractor.

Using the MFDFA analysis, in the present study, we have shown the existence of scale invariant characteristics of the time series X of the system obtained for different a_2 values by finding the behavior of Hürst exponent H_q (Fig. 9a,b) and the singularity spectrum (D_q vs h_q) in each cases (Fig. 10a,b). The detection of multi-fractality in a time series provides a basis for the intermittent behavior in the time series of the species X. It is to be noted that crashes in super predator Z causes significant increase/ swings in the population Y and X whereas the increase in Z results in the damping of the tendency for increase in Y and X till Y crashes. This will subsequently results in crashes in Z and X reaching a maximum and the process cycle begins again. Since the timing of the sequence of such events vary erratically, intermittency sets in. The scale dependent measure of eq.(18) is described by the scaling exponent H_q which numerically defines the power law relation of the intermittent periods with large variation when q is positive and periods with small variation when q is negative. The observed behavior of the multi-fractal spectrum and other foregoing parameters clearly suggests multi-fractal nature of the considered time series data and also suggest a long-range correlation in the data.

Acknowledgement: Authors are thankful to Guru Gobind Singh Indraprastha University, Delhi (India) for providing research facilities and financial support.

Conflicts of Interest: The authors declare no conflict of interest.

References

[1] D. L. Baho, M. N. Futter, R. K. Johnson & D. G. Angeler (2015). Assessing temporal scales and patterns in time series: Comparing methods based on redundancy analysis. *Ecological Complexity*, *22*, 162–168. https://doi.org/10.1016/j.ecocom.2015.04.001.

[2] L. Becks, F. M.Hilker, H. Malchow, K. Jügens & H. Arndt (2005). Experimental demonstration of chaos in a microbial food web. *Nature*, *435*(7046), 1226–1229. https://doi.org/10.1038/nature03627.

[3] J. R. Beddington (1975). Mutual interference between parasites or predators and its effect on searching efficiency. *Journal of Animal Ecology*, *44*(1), 331–340. https://doi.org/10.2307/3866.

[4] L. Berec (2010). Impacts of foraging facilitation among predators on predator-prey dynamics. *Bulletin of Mathematical Biology*, *72*(1), 94–121. https://doi.org/10.1007/s11538-009-9439-1.

[5] S. Bhaduri, R. Das & D. Ghosh (2016). Non-invasive detection of Alzheimer's disease- multifractality of emotional speech. *J. Neurology and Neuroscienc*, *7*(2), 84. https://doi.org/10.21767/2171-6625.100084.

[6] N. K. Bhatraju & M. Das (2014). On multifractality and synchronization of nonlinear stellar pulsators. *Astrophysics and Space Science*, *352*(1), 83–94. https://doi.org/10.1007/s10509-014-1887-x.

[7] V. Castellanos & R. E. Chan-Loṕez (2017). Existence of limit cycles in a three level trophic chain with Lotka-Volterra and Holling type II functional responses. *Chaos Solitons & Fractals*, *95*, 157–167. https://doi.org/10.1016/j.chaos.2016.12.011.

[8] P. Castiglioni, D. Lazzeroni, P. Coruzzi & A. Faini (2018). Multifractal-multiscale analysis of cardiovascular signals: A DFA- based characterization of blood pressure and heart-rate complexity by gender. *Hindawi Complexity*, *2018*(Article ID: 4801924, 15 pages). https://doi.org/10.1155/2018/4801924.

[9] M. Das, A. Bhattacharjee, N. K. Bhatraju, M. Yuasa & L. M. Saha (2012). Cooperative dynamics of coupled neuron model and multifractality. *Bulletin of Callcutta Mathematical Society*, *104*(561–590). https://doi.org/10.1016/j.cnsns.2016.10.022.

[10] D. DeAngelis, R. A. Goldstein & R. V. O'Neill (1975). A model for tropic interaction. *Ecology*, *56*(4), 881–892. https://doi.org/10.2307/1936298.

[11] Q. Dong, Y. Wang & P. Li (2017). Multifractal behavior of an air pollutant time series and the relevance to the predictability. *Environmental Pollution*, *222*, 444–457. https://doi.org/10.1016/j.envpol.2016.11.090.

[12] A. Garmendia & A. Salvador (2007). Fractal dimension of birds population sizes time series. *Mathematical Biosciences*, *206*(1), 155–171. https://doi.org/10.1016/j.mbs.2005.03.014.

[13] J. Ghosh, B. Sahoo & S. Poria (2017). Prey-predator dynamics with prey refuge providing additional food to predator. *Chaos, Solitons & Fractals*, *96*, 110–119. https://doi.org/10.1016/j.chaos.2017.01.010.

[14] A. L. Goldberger, L. A. Amral, J. M. Hausdorff, P. C. Ivanov & C. K. Peng (2002). Fractal dynamics in physiology: Alterations with disease and aging. *Proceedings of the National Academy of Sciences of the United States of America*, *99*(suppl 1), 2466–2472. https://doi.org/10.1073/pnas.012579499.

[15] A. Hastings & T. Powell (1991). Chaos in a three-species food chain. *Ecology*, *72*(3), 896–903. https://doi.org/10.2307/1940591.

[16] C. S. Holling (1959). Some characteristics of simple types of predation and parasitism. *The Canadian Entomologist*, *91*(7), 385–398. https://doi.org/10.4039/Ent91385-7.

[17] E. A. F. Ihlen (2012). Introduction to multifractal detrended fluctuation analysis in Matlab. *Frontiers in Physiology*, *3*, 141. https://doi.org/10.3389/fphys.2012.00141.

[18] E. A. F. Ihlen (2014). Multifractal analyses of human response time: Potential pitfalls in the interpretation of results. *Frontiers in Human Neuroscience*, *8*, 523. https://doi.org/10.3389/fnhum.2014.00523.

[19] J. W. Kantelhardt, S. A. Zschieger, E. B. Koscienly, S. Halvin, A. Bunde & H. E. Stanley (2002). Multifractal detrended fluctuation analysis of nonstationary time series. *Physica A: Statistical Mechanics and its Applications*, *316*(1-4), 87–114. https://doi.org/10.1016/S0378-4371(02)01383-3.

[20] A. Klebanoff & A. Hastings (1994). Chaos in three species food chains. *Journal of Mathematical Biology*, *32*, 427–451. https://doi.org/10.1007/BF00160167.

[21] R. F. Leonarduzzi, G. Schlotthauer & M. E. Torres (2011). Short-time multifractal analysis: Application to biological signals. *Journal of Physics: Conference Series*, *313 012012*(1-8). https://doi.org/10.1088/1742-6596/313/1/012012.

[22] C. Letellier & M. A. Aziz-Alaoui (2002). Analysis of dynamics of realistic ecological model. *Chaos Soliton & Fractals*, *13*(95-107). https://doi.org/10.1016/S0960-0779(00)00239-3.

[23] A. J. Lotka (1925). *Elements of physical biology*. Williams and Wilkins, Baltimore.

[24] S. Lv & M. Zhao (2008). The dynamic complexity of a three species food chain model. *Chaos Solitons & Fractals*, *37*(1469-1480). https://doi.org/10.1016/j.chaos.2006.10.057.

[25] P. Mali & A. Mukhopadhyay (2015). Long-range memory and multifractality in gold markets. *Physica Scripta*, *90(3)*(Article ID: arXiev:1505.08136v1 [q-fin.ST], 21 pages). https://doi.org/10.1088/0031-8949/90/3/035209.

[26] S. Mandal, T. Roychowdhury, K. Chirom, A. Bhattacharya & R. K. B. Singh (2017). Complex multifractal nature in Mycobacterium tuberculosis genome. *Scientific Reports*, *7*(Article ID: 46395, 13 pages). https://doi.org/10.1038/srep46395.

[27] B. Mandelbrot (1981). *The fractal geometry of nature*. W.H.Freeman and Company, New York.

[28] K. McCann, A. Hastings & G. Huxel (1998). Weak trophic interactions and the balance of nature. *Nature*, *7*(794-798). https://doi.org/10.1038/27427.

[29] A. B. Medvinsky, B. V. Adamovich, A. Chakraborty, E. Lukyanova, T. M. Mikheyeva, N. I. Nurieva, N. P. Radchikova, A. V. Rusakov & T. V. Zhukova (2015). Chaos far away from edge of chaos: A recurrence quantification analysis of plankton time series. *Ecological Complexity*, *23*(61-67). https://doi.org/10.1016/j.ecocom.2015.07.001.

[30] R. M. Montes, R. I. Perry, E. Pakhomov, A. M. Edwards & J. A. Boutillier (2012). Multifractal patterns in the daily catch time series of smooth pink shrimp (Pandalus jordani) from the west coast of Vancouver Island, Canada. *Canadaian Journal of Fisheries and Aquatic Sciences*, *69*(398-413). https://doi.org/10.1139/f2011-156.

[31] R. M. Montes-Aste (2015). *Fractal Analysis of Fisheries and Environmental Time Series for the Development of Early Warning Indicators*. PhD thesis, The University of British Columbia, Vancouver.

[32] A. F. Nindjin, M. A. Aziz-Alaoui & M. Cadivel (2006). Analysis of a predator-prey model with modified Leslie-Gower and Holling-type II schemes with time delay. *Nonlinear Analysis: Real World Applications*, *7*(1104-1118). https://doi.org/10.1016/j.nonrwa.2005.10.003.

[33] N. Pal, S. Samanta & J. Chattopadhyay (2014). Revisited Hastings and Powell model with omnivory and predator switching. *Chaos Solitons & Fractals*, *66*(58-73). https://doi.org/10.1016/j.chaos.2014.05.003.

[34] S. N. Raw, P. Mishra, R. Kumar & S. Thakur (2017). Complex behavior of prey-predator system exhibiting group defense: A mathematical modeling study. *Chaos Solitons & Fractals*, *100*(74-90). https://doi.org/10.1016/j.chaos.2017.05.010.

[35] L. A. Saravia (2014). mfSBA: Multifractal analysis of spatial patterns in ecological communities. *F1000research*, *3:14*(1-13). https://doi.org/10.12688/f1000research.3-14.v2.

[36] L. A. Saravia (2015). A new method to analyse species abundances in space using generalized dimensions. *Methods in Ecology and Evolution*, *6*(1298-1310). https://doi.org/10.1111/2041-210X.12417.

[37] N. Scafeta, L. Griffin & B. West (2003). Hölder exponent spectra for human gait. *Physica A: Statistical Mechanics and its Application*, *328*(561-583). https://doi.org/10.1016/S0378-4371(03)00527-2.

[38] L. Seuront & H. E. Stanley (2014). Anomalous diffusion and multifractality enhance mating encounters in the ocean. *PNAS*, *111*(2206-2211). https://doi.org/10.1073/pnas.1322363111.

[39] L. Stone & D. He (2007). Chaotic oscillations and cycles in multi-trophic ecological systems. *Journal of Theoretical Biology*, *248*(382-390). https://doi.org/10.1016/j.jtbi.2007.05.023.

[40] G. Sugihara & R. M. May (1990). Application of fractals in ecology. *Trends in Ecology and Evolution*, *5*(79-86). https://doi.org/10.1016/0169-5347(90)90235-6.

[41] L. Telesca, G. Colangelo & V. Lapenna (2005). Multifractal variability in geoelectrical signals and correlations with seismicity: A study case in Southern Italy. *Natural Hazards and Earth System Sciences*, *5*(673-677). https://doi.org/10.5194/nhess-5-673-2005.

[42] P. Turchin (2003). *Complex population dynamics; a theoretical / empirical synthesis*. Princeton University Press, Princeton.

[43] V. Volterra (1926). Fluctuations in the abundance of a species considered mathematically. *Nature*, *118*(558-560). https://doi.org/10.1038/118558a0.

[44] A. Wolf, J. B. Swift, H. L. Swinney & J. A. Vastano (1985). Determining Lyapunov exponents from a time series. *Physica D: Nonlinear Phenomena*, *16*(*3*)(285-317). https://doi.org/10.1016/0167-2789(85)90011-9.

[45] L. Zhao, L. Wei, C. Yang, J. Han, Z. Shu & Y. Zou (2017). Multifractality and network analysis of phase transition. *PLoS ONE*, *12*(*1*)(Article ID: e0170467, 23 pages). https://doi.org/10.1371/journal.pone.0170467.